Petro TROKHIMCHUCK

Ph.D., Associate Professor Associate Professor at Department of A.V. Svidzynskiy's Theoretical and Computer Physics, Lesya Ukrainka Volyn National University, 13 Volya Ave., Lutsk, Ukraine, 43025
ORCID ID: *0000-0003-2737-0506*
SCOPUS-AUTHOR ID: *8383601100*

MAIN PROBLEMS OF MODELING LASER-INDUCED BREAKDOWN OF MATTER

The main problems of modeling the laser-induced breakdown of matter are discussed. We show that this problem must be represented as resolution of famous Newtonian phrase: "Optics studies the processes associated with the transition of light into matter and matter into light." Short analysis of main kinetic and dynamic processes is analyzed. Photoinduced and photochemical processes are represented kinetic phenomena. Thermal and plasma processes – dynamic phenomena. Unlike electrical breakdown, which can be superficial, laser-induced breakdown occurs in a medium that is transparent to the incident radiation. Therefore, we present the main differences between electrical and laser-induced breakdown. These processes are accompanied of phase transformations of irradiated matter. These processes have saturation nature. We show that these process have cascade nature. Therefore, basic problem of modeling is find the corresponding chain of interconnected phenomena, which are generated in the process of interaction the light and matter. Short analysis of corresponding models, which are used for the explanation of main peculiarities of electrical and laser-induced breakdown, are represented. These phenomena have threshold nature. Therefore, we selected experimental data of creation laser-induced optical breakdown for silicon carbide and potassium chloride. The proper cascade model was created. This model includes next stages: diffraction stratification (modifid model of Rayleygh rings); generation of Cherenkov radiation on each cone of corresponding diffraction ring (synthesized Golub and Niels and Aage Bohrs models); interference of short-wave part of Cherenkov radiation; optical breakdown in maximum of this interferograms. At the same time, the emergence of nanocavities in breakdown channels was explained on the basis of a modified Rayleigh model. It was also established that this shock process has electromagnetic nature.
Key words: laser, optical breakdown, Relaxed Optics, cascade processes, shock processes, modeling.

Петро ТРОХИМЧУК

кандидат фізико-математичних наук, доцент, доцент кафедри теоретичної та комп'ютерної фізики імені А. В. Свідзинського, Волинський національний університет імені Лесі Українки, просп. Волі, 13, м. Луцьк, Україна, 43025
ORCID ID: *0000-0003-2737-0506*
SCOPUS-AUTHOR ID: *8383601100*

ОСНОВНІ ПРОБЛЕМИ МОДЕЛЮВАННЯ ЛАЗЕРНО-ІНДУКОВАНОГО ОПТИЧНОГО ПРОБОЮ РЕЧОВИНИ

Обговорюються основні проблеми моделювання лазерно-індукованого руйнування речовини. Ми показуємо, що ця проблема повинна бути представлена як розв'язання знаменитої фрази Ньютона: «Оптика вивчає процеси, пов'язані з переходом світла в матерію і матерії у світло». Проаналізовано короткий аналіз основних кінетичних і динамічних процесів. Фотоіндуковані та фотохімічні процеси представлені кінетичними явищами. Теплові та плазмові процеси – динамічні явища. На відміну від електричного пробою, який може бути поверхневим, лазерний пробій відбувається в середовищі, прозорому для падаючого випромінювання. Тому ми представляємо основні відмінності між електричним та лазерним пробоєм. Ці процеси супроводжуються фазовими перетвореннями опроміненої речовини. Також вони мають характер насичення. Показано, що ці процеси мають каскадний характер. Тому основною задачею моделювання є пошук відповідного ланцюга взаємопов'язаних

явищ, які генеруються в процесі взаємодії світла та матерії. Подано короткий аналіз відповідних моделей, які використовуються для пояснення основних особливостей електричного та лазерного пробою. Ці явища мають пороговий характер. Тому ми відібрали експериментальні дані створення лазерно-індукованого оптичного пробою для карбіду кремнію та хлориду калію. Була створена відповідна каскадна модель. Ця модель включає такі етапи: дифракційна стратифікація (модифікована модель кілець Релея); генерація черенковського випромінювання на кожному конусі відповідного дифракційного кільця (синтезована модель Голуба та Н. та О. Борів); інтерференція короткохвильової частини черенковського випромінювання; оптичний пробій в максимумі цієї інтерферограми. Водночас появу нанопорожнин у каналах пробою було пояснено на основі модифікованої моделі Релея. Також встановлено, що цей ударний процес має електромагнітну природу.

Ключові слова: *лазер, оптичний пробій, релаксаційна оптика, каскадні процеси, ударні процеси, моделювання.*

INTRODUCTION

Problems of the observation the laser-induced optical breakdown and shock processes in matter as Nonlinear (NLO) and Relaxed (RO) Optical processes are connected with acoustic (thermal) and electromagnetic (plasma and Nonlinear optical) nature (Shen, 2003; Trokhimchuck, 2020; Trokhimchuck, 2022). These processes may be connected with diffractive stratification of laser beam, self-focusing, self-trapping, generation of supercontinuum radiation (ordered – Cherenkov radiation, and disorder – plasma radiation) (Trokhimchuck, 2020; Trokhimchuck, 2022).

The first models were created similar to the electric breakdown of matter (Lehr, 2017). Unlike laser breakdown, electrical breakdown can be both bulk and surface (current lacing in semiconductors). The main problems of these models were to find the mechanisms of electron avalanche generation. Then thermal and plasma models were developed.

For laser-induced optical breakdown of the medium, the problem of electron generation must be associated with photochemical excitation and reactions that lead, as a rule, to phase transitions of the irradiated substance. Therefore, we must find possible channels of transformation initial laser radiation to ended irradiation or other action, which is generated the breakdown.

These phenomena are having the threshold and saturation nature and full process is complex cascade with few stages of various phenomena.

Therefore, main problem of this paper is selection the most significant concentrations and processes that give the greatest contribution to the final effect.

EXPERIMENTAL DATA

A good review of experimental results on the electrical breakdown of the medium is given in (Okada, 2009; Okada, 2012; Yablonovich, 1971).

A number of typical destructions of real transparent media have been experimentally revealed (Okada, 2009; Okada, 2012):

– destruction of the surface of glass or quartz structural parts (plates, prisms, lenses) with the appearance of opaque macroscopic local formations;

– destruction of thin-film metal and dielectric mirror coatings in the presence of an opaque defect in the coating or the appearance on the surface of dust or other opaque macroscopic local formations;

– destruction inside the glass, crystals, active elements that occur on macroscopic local impurities or defects that are inside this environment.

More complex experimental data, which are included optical breakdown, were received in (Okada, 2009; Okada, 2012) (Fig. 1).

Sectional area of receiving structures was ~ 22 μm, the depth of ~ 50 μm. As seen from Fig. 1 (c) we have five stages disordered regions, which are located at a distance from 2 to 4 μm apart vertically (Okada, 2009; Okada, 2012). Branches themselves in this case have a thickness from 150 to 300 nm. In this case there are lines in the irradiated nanocavity spherical diameter of from 10 nm to 20 nm. In this case irradiated structures have crystallographic symmetry of the initial structure.

In this case diffraction processes may be generated in two stages: 1 – formation of diffraction rings of focused beams (Trokhimchuck, 2020) and second – formation of diffracting gratings in the time of redistribution of second-order Cherenkov radiation (Trokhimchuck, 2020). Second case is analogous to the creation of self-diffraction gratings in NLO, but for Fig. 1 (c) and Fig. 1 (e) our gratings are limited by Much cone of Cherenkov radiation. Roughly speaking only Fig. 1 (e) – (g) are represented "clean" breakdown.

Two damages region in a crystal with moderately high density of inclusions were received in (Yablonovich, 1971) for *KCl* after irradiation by CO_2-lase pulses (wavelength 10,6 μm, duration of pulse 30 ns). The laser was known to be operating in the lowest-order transverse Gaussian mode. There were several longitudional modes, however,
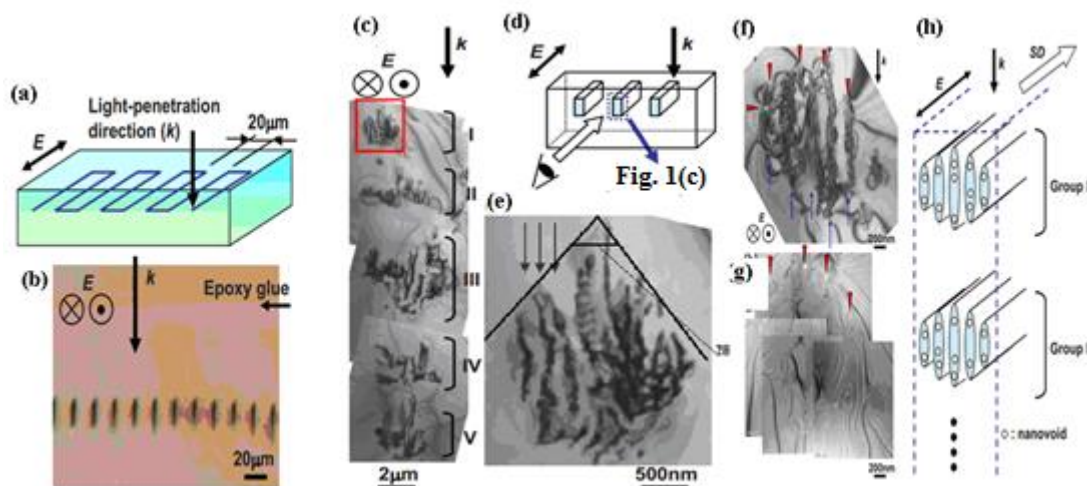
Fig 1. (a) Schematic illustration of the laser irradiated pattern. The light propagation direction (k) and electric field (E) are shown. (b) Optical micrograph of the mechanically thinned sample to show cross sections of laser-irradiated lines (200 nJ/pulse). (c) Bright-field TEM image of the cross section of a line written with pulse energy of 300 nJ/pulse. (d) Schematic illustration of a geometric relationship between the irradiated line and the cross-sectional micrograph. (e) Magnified image of a rectangular area in (c). Laser-modified layers with a spacing of 150 nm are indicated by arrows. (f) Bright-field TEM image of a portion of the cross section of a line written with a pulse energy of 200 nJ/pulse. (g) Zero-loss image of a same area as in (f) with nanovoids appearing as bright areas. Correspondence with (f) is found by noting the arrowheads in both micrographs. (h) Schematic illustrations of the microstructure of a laser modified line. Light-propagation direction (k), electric field (E), and scan direction (SD) are shown. Only two groups (groups I and II) of the laser-modified microstructure are drawn (Okada, 2009; Okada, 2012)

which contributed a time structure to the pulse, periodic at the cavity round-trip time. The phase relationships between the longiotudional modes varied from shot to shot, changing the details of the time structure and causing the peak of the envelope to fluctuate by ±15% (Yablonovich, 1971). These results are presented in Fig. 2 (Yablonovich, 1971).

Successive laser shot (1/sec) were focused into bulk single crystals using a 1–inch focal length "Irtran 2" lens. The breakdown was monitored by observing the visible light from the focal region and by examining the damaged region under the microscope. It was found that most of the crystals suffered some damage even at relatively low power levels. The threshold of this type of damage varied by an order magnitude from one position in the crystal to another. At any particular energy level, damage would occur on the first laser shot or not at all.

Fig. 2(a) shows that spatial inhomogeneities are in fact inclusions ((Yablonovich, 1971). The damage bubbles occur randomly near, not necessarily in, the tiny focal volume. At a well-defined power threshold, an elongated pointed bubble forms, its vertex falling at the focus (Fig. 2(b)). This power level is regarded ass the bulk intrinsic breakdown threshold. Its value is reproducible in crystals from different manufacturers, with inclusions or without. When no inclusion-free samples of a compound were available, the considerations mentioned above were used to determine the dielectric strength ((Yablonovich, 1971).

MODELING AND DISCUSSIONS

Main characteristioc of electrical breakdown is critical value of voltage, which is necessary for realization of this process (Lehr, 2017; Fröhlich, 1946; Wang, 2012). Depending on the conditions of the experiment, a plasma or thermal breakdown mechanism can be realized there. These theories were transferred to the problem of laser-induced optical breakdown [Shen, 2003; Trokhimchuck, 2020). But with the help of these theories, it is difficult to explain the experimental results shown in Fig. 1 and Fig. 2.

For the optical breakdown of a solid body, each atom needs to be given Seitz energy (the sum of the
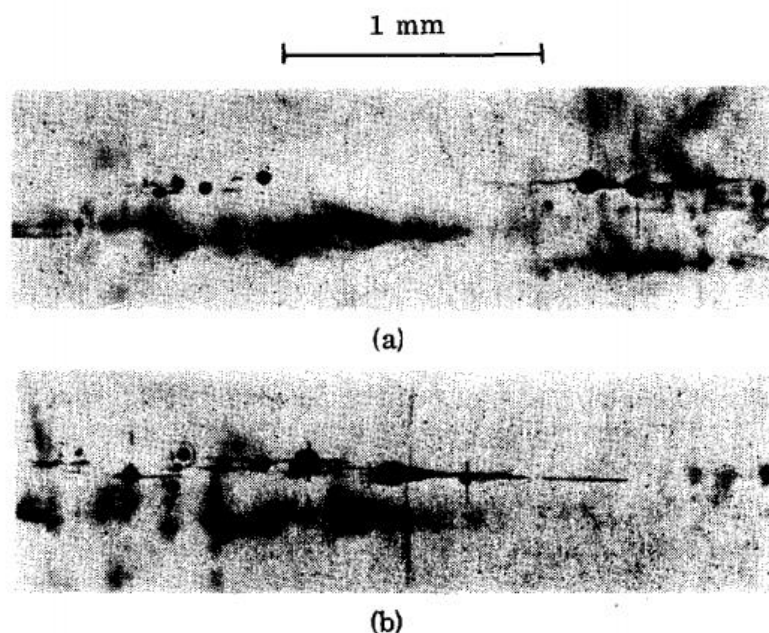
Fig. 2. Two damages region in a crystal *KCl* with moderately high density of inclusions. The round black objects are bubbles. The radiation, incident from left to right, was yust at the intrinsic breakdown threshold. In one case (a) there was damage only at the inclusions. In (b), intrinsic breakdown occurred as evidenced by the pointed bubble. The straight lines represent cleavage (Yablonovich, 1971)

energies of the chemical bonds of our atom with its nearest neighbors) (Trokhimchuck, 2020). But for this, we must "organize" the irradiation process in such a way that this mechanism is implemented. It is here that we must remember Newtonian phrase: "Optics studies the processes associated with the transition of light into matter and matter into light."

Based on this, we chose the following chain of processes: diffraction stratification, Cherenkov radiation by each diffraction cone (the components of the Mach cone of this radiation are perpendicular to the components of the diffraction cone); interference of the short-wave part of this radiation; optical breakdown occurs in the maxima of the interference pattern.

In addition, an adapted Rayleigh model was created to simulate the size and shape of the nanovoids formed in the breakdown channels (Fig. 1 h)).

Diffraction stratification was modeled with help Rayleygh rings. Diameter of corresponding ring is equaled (Trokhimchuck, 2020; Trokhimchuck, 2022)

$$d_{ndif} = n\lambda \qquad (1)$$

where n – number of ring, λ – wavelength of initial laser irradiation.

The number of diffraction rings may be determined from experimental data (five for Fig. 1 c) and ~ 7 for Fig. 2. This number may be determined theoretically with Durbin model (Trokhimchuck, 2020).

This leads to a local refractive-index change $\Delta n(\rho, z)$ in the medium seen by the laser and a corresponding phase shift $\Delta\psi$ of the beam traversing the medium of thickness d:

$$\Delta\psi(\rho) = \frac{2\pi}{\lambda} \int_{-d/2}^{d/2} \Delta n(\rho, z)\, dz, \qquad (2)$$

where ρ is transverse position in the beam. For this geometry $\Delta n(\rho, z)$ and $\Delta\psi(\rho)$ also correspond, respectively, to the induced local birefringence and overall phase retardation between ordinary and extraordinary rays. For a single transverse-mode laser, and supposing the elastic response of the liquid crystal to be isotropic, we expect that $\Delta\psi(\rho)$ is cylindrically symmetric in the form of a bump peaked at $\rho = 0$. We assume, for simplicity, that (Trokhimchuck, 2020)

$$\Delta\psi(\rho) = \Delta\psi_0 \exp\left(-2\rho^2 / a^2\right), \qquad (3)$$

with a being a constant. Then, as is seen in Fig. 2.4, for each point, say ρ_1, on the $\Delta\psi(\rho)$ function, there always exists another point ρ_2 with the

same slope. Since $d\Delta\psi/d\rho = k_\perp$, the radiation fields from the regions around ρ_1 and ρ_2 have the same wave vector and can interfere. Maximum constructive or destructive interference occurs when $\Delta\psi(\rho_1) - \Delta\psi(\rho_2) = m\pi$, m being an even or odd integer, respectively, with the resulting appearance of diffraction rings. Thus, if $\Delta\psi_0 \gg 2\pi$, multiple diffraction rings are expected, and the total number of rings N can be estimated from the relation

$$N \cong \Delta\psi_0 / 2\pi. \qquad (4)$$

The outermost ring should come from radiation from the region ρ around the inflection point on the $\Delta\psi(\rho)$ curve, and its half-cone angle θ_m can be calculated from (Trokhimchuck, 2020)

$$\theta_m \cong \left(\frac{d\Delta\psi}{d\rho}\right)_{max} \Big/ \left(2\pi/\lambda\right). \qquad (5)$$

For modeling conic Cherenkov radiation we used synthesis microscopin Niels and Aage Bohrs and macroscopic Golub models (Trokhimchuck, 2020). This models allow to unite geometry characteristics and changed of lasser-induced nonlinear characteristics matter in one formula. In this case the Cherenkov radiation is result of nonlinear polarization of medium.

The angle 2θ in the vertex of an angle of Fig. 1 (e) is double Cherenkov angle.

Macroscopic relation with Snell's law, gives the Cherenkov relation (Golub formula) (Trokhimchuck, 2020).

$$cos\theta = c / n_2(\omega)V. \qquad (6)$$

Where c – light velocity, $n_2(\omega)$ – nonlinear refraction undex, V – velocity of nonlinear polarizaion of natter.

The microscopic mechanism of laser-induced Cherenkov radiation is expansion and application of Niels and Aage Bohrs microscopic theory of Cherenkov radiation as part of deceleration radiation on optical case (Trokhimchuck, 2020). For optical case the Bohrs hyperboloid must be changed on Gaussian distribution of light for mode TEM_{00} or distribution for focused light of laser beam (Trokhimchuck, 2020). In this case Cherenkov angle may be determined from next formula

$$\theta_{Ch} + \alpha_{ir} = \pi/2 \text{ or } \theta_{Ch} = \pi/2 - \alpha_{ir}, \qquad (7)$$

where α_{ir} – angle between tangent line and direction of laser beam.

Angle α_{ir} was determined from next formula (Trokhimchuck, 2020)

$$\tan\alpha_{ir} = d_b / l_{sf}, \qquad (8)$$

where d_b – diameter of laser beam, (7 mm), l_{sf} – length of self-focusing. In our case α_{ir} is angle of self-focusing.

This formula is approximate for average angle α_{ir}.

The Golub formula (6) was used for the determination product $n_2(\omega)V_{nl\ pol}$. Thereby microscopic modified Bohrs theory and macroscopic Golub model are mutually complementary methods (Trokhimchuck, 2020).

The distance between diffraction spots and proper moving foci may be determined with help next formula (Trokhimchuck, 2020)

$$l_{nf} = \frac{d_{ndif}}{2\tan\frac{\varphi}{2}}. \qquad (9)$$

The influence of multi-photon absorption on the dielectric breakdown threshold was noted as early as in the Fröhlich (Fröhlich, 1946; Wang, 2012).

For the estimation basic peculiarities of energy distribution in Mach cone of Fig. 1 c) may be used next formula [2]

$$E_{1ob} = \frac{\pi^2}{4}\left(\sum_{i=1}^{5} n_{iav}^2 l_{iav}\right) r^2 N_{aSiC} E_{Zth}, \qquad (10)$$

where n_{iav} – average visible number of filaments in proper group of cascade, l_{iav} =1000 nm – average length of filaments in proper group of cascade, r = 10 nm – average radius of filament, N_a – atom density of 4H-SiC.

Therefore, summary energy of breakdown E_{1ob} for silicon carbide is equaled 23.3 nJ or $\sim 8\%$ from pulse energy or $\sim 30\%$ from the effective absorbed energy of pulse. In this case we have more high efficiency of transformation initial radiation to "irreversible" part of Cherenkov radiation. For potassium chloride from 24.2 mJ (Fig. 2a)) to 34.8 mJ (Fig. 2 b)) or from 11,6 to 17,4 percents from initial irradiation [2]. This is due to the dependence of the sizes of diffraction cones and other geometrical dimensions on the wavelength of irradiation (formulas (1) and (9)).

For the determination sizes and forms of nanovoids (Fig. 1 h)) we used the Rayleygh model,

which was adapted for electromagnetic case (Trokhimchuck, 2020).

For the estimations of maximal radius of nanovoids we must use modified Rayleygh formula (Trokhimchuck, 2020)

$$R_{max} = \frac{2R}{0.915r} \sqrt{\frac{E_{ir}}{\pi \tau_{ir} cE}}, \qquad (11)$$

where T_c – the time of creation the nanovoid (bubble), R is radius of nanovoid, r – radius of irradiated zone, E – Young module, E_{ir} – energy of one pulse. τ_{ir} – duration of pulse (Trokhimchuck, 2020).

If we substitute $r = 250$ nm, $R = 10$ nm, E=600 GPa [176, 212, 273], E_{ir}=130 nJ, $\tau_i = 130$ ps, c=3·10⁸ m/s, than have R_{max}=11 nm.

The velocity of shock waves for femtosecond regime of irradiation is less as speed of sound. But we have two speeds of sound in elastic body:

longitudinal ϑ_{ls} and transversal ϑ_{ts} (Trokhimchuck, 2020). Its values are determined with next formulas

$$\vartheta_{ls} = \sqrt{\frac{E(1-\nu)}{\rho_o (1+\nu)(1-2\nu)}}, \text{ and } \vartheta_{ts} = \sqrt{\frac{E}{2\rho_o (1+\nu)}}, \quad (12)$$

where ν – Poisson's ratio (Trokhimchuck, 2020). The ratio between of these two speeds is equaled

$$\alpha = \frac{\vartheta_{ts}}{\vartheta_{ls}} = \sqrt{\frac{(1-2\nu)}{2(1-\nu)}}. \qquad (13)$$

But this ratio must be true for shock waves too. Therefore, for silicon carbide for $\nu = 0,45$ [2] $\alpha = 0,33$. Roughly speaking last ratio is determined the step of ellipsoidal forms of our nanovoids (Fig. 1 (h)).

CONCLUSIONS

1. A comparative analysis of electric and laser-induced breakdown of solids (experimental data and modelling) was carried out.

2. It is shown that the laser-induced optical breakdown of matter has a cascade nature.

3. The presented cascade model, which includes diffraction stratification, generation of Cherenkov radiation, interference of the short-wavelength region of this radiation, and actual optical breakdown, allows to explain the main features of this process.

4. It is shown that the formation of nanocavities is caused by electromagnetic shock processes.

5. In general, the laser-induced optical breakdown itself from a microscopic point of view is caused by multiphoton absorption and the saturation effect of the excitation of the irradiated region.

REFERENCES:

1. Fröhlich, H. H. (1946) On the theory of dielectric breakdown in solids. Proc. Roy. Soc. A, vol. 187, pp. 521–532.

2. Lehr, J., Ron, P. (2017) Electrical Breakdown in Solids, Liquid, and Vacuum. Ch. 9 in: Foundation of Pulse Power Technology. New York a. o.: Wiley-Interscience, pp. 439–497.

3. Okada T., Tomita T., Matsuo S., Hashimoto S., Ishida Y., Kiyama S., Takahashi T. (2009) Formation of periodic strain layers associated with nanovoids inside a silicon carbide single crystal induced by femtosecond laser irradiation. J. Appl. Phys., v. 106, p. 054307, 5 p.

4. Okada T., Tomita T., Matsuo S., Hashimoto S., Kashino R., Ito T. (2012) Formation of nanovoids in femtosecond laser irradiated single crystal silicon carbide. Material Science Forum, vol. 725, pp.19–22.

5. Shen, Y. R. (2003) The principles of Nonlinear Optics. New York a. o.: Wiley-Interscience, 563 p.

6. Trokhimchuck, P. P. (2020) Laser-induced optical breakdown of matter: retrospective and perspective./ Advances in Engineering Technology, vol. 4, part 7. New Dehly : AkiNik Publications, pp. 101–132.

7. Trokhimchuck, P.P. (2022) Diffraction: Concepts and Applications. In:Recent Review and Research in Physics. Ed. Jayminkumar Rajanikant Ray, S.S. Sharma, vol. 1, ch. 3. New Dehly : AkiNik Publications, pp. 37–67.

8. Wang H., Zeng Zh. (2012) Electric Breakdown Model for Super-Thin Polyester Foil, ch. 14, pp. 359-376. INTECH, doi: 10.5772/48478, Corpus ID: 34410888.

9. Yablonovich, E. (1971) Optical Dielectric Srength of AlkaliHalide Crystalls Obtained by Laserinduced Breakdown. Appl. Phys. Lett., vol.19, is.11, P. 495–497.